

AXAF Calibration: The HXDS Flow Proportional Counters

B. J. Wargelin, E. M. Kellogg, W. C. McDermott, I. N. Evans, and S. A. Vitek

Smithsonian Astrophysical Observatory, MS-27
Cambridge, Massachusetts 01238 USA

ABSTRACT

The design, performance, and calibration of the seven Flow Proportional Counters (FPCs) used during AXAF ground calibration are described. Five of the FPCs served as Beam Normalization Detectors (BNDs), and two were used in the telescope focal plane in combination with a set of apertures to measure the point response functions and effective areas of the AXAF mirrors and transmission gratings. The BNDs also provide standards for determining the effective areas of the several telescope/grating/flight-detector combinations.

With useful energy resolution and quantum efficiency over the entire 100-eV to 10-keV AXAF energy band, the FPCs provided most of the data acquired during AXAF calibration. Although the principles of proportional counter operation are relatively simple, AXAF's stringent calibration goals require detailed calibration and modeling of such effects as window-support-wire obscuration, window deformation between the support wires, electron diffusion and avalanche processes, gain nonuniformities, and gas pressure and temperature variations. Detector aperture areas and signal processing deadtime must also be precisely determined, and detector degradation during the many months of AXAF calibration must be prevented.

The FPC calibration program is based on measurement of individual components (such as window transmission and aperture size) and the relative quantum efficiencies of complete detector systems, as well as absolute QE calibration of selected detectors at the BESSY synchrotron, an X-ray source of precisely known intensity.

Keywords: AXAF, calibration, proportional counters, X-ray detectors

1. INTRODUCTION

The HRMA X-ray Detection System (HXDS) was used for ground-based calibration of the AXAF High Resolution Mirror Assembly (HRMA), transmission gratings, and flight detectors at the Marshall Space Flight Center's X-Ray Calibration Facility (XRCF). It consists of seven Flow Proportional Counters (FPCs), two germanium Solid State Detectors (SSDs),^{1,2} and one microchannel-plate High Speed Imager (HSI),³ plus associated hardware such as apertures and translation stages, all controlled by the X-ray Detection And Control System (XDACS) software. The ten detectors are grouped into three assemblies:

BND-500 The Beam Normalization Detectors at Building 500, located 38 m from the X-ray source system and consisting of one fixed-position SSD and one FPC mounted on translation stages to allow two-dimensional beam uniformity mapping.

BND-H The Beam Normalization Detectors at the HRMA, located 525 m from the X-ray source and consisting of four FPCs (one of them a mapper) arrayed just in front of the HRMA on its periphery.

HXDA The HXDS X-ray Detector Assembly, positioned in the focal plane of the HRMA, consisting of the HSI, the second SSD, and an FPC (with a never-used backup) and its set of 34 apertures, all mounted on translation stages with three-dimensional positioning capability.

The BND-500 and BND-H detectors were used throughout the two phases of AXAF calibration for X-ray beam intensity monitoring and uniformity mapping, and for normalization of the focal plane detectors. During Phase 1, the HXDA was used in the focal plane to calibrate the HRMA and gratings more thoroughly than could be done with the flight detectors; during Phase 2, the HXDA was replaced by the High Resolution Camera (HRC) and AXAF CCD Imaging Spectrometer (ACIS) flight detectors.

The HXDS is designed to measure the effective area (in cm^2) of all combinations of the HRMA, gratings, and ACIS and HRC to of order 1% over the entire AXAF energy band from 100 eV to 10 keV, and to measure the focusing properties (primarily the point response function and encircled energy curve) of the HRMA and gratings with similar accuracy on scales as small as $5 \mu\text{m}$. Together, the HXDS detectors provide a complementary set of functionalities for these tasks: the FPCs with their wide energy range, moderate energy resolution, and large collecting area; the SSDs with their excellent energy resolution, stable gain, and $\sim 100\%$ quantum efficiency at high energies; and the HSI with its imaging capabilities and spatial resolution of $17 \mu\text{m}$. The focal plane SSD and FPC, although possessing no intrinsic spatial resolution, could also be used to study the structure of the focused beam by appropriate use of their associated apertures. A comparison of detector quantum efficiencies is shown in Figure 1.

2. DESIGN AND OPERATION

The entire AXAF energy range was studied during calibration at the XRCF. X rays were provided by a set of four sources in the X-ray Source System,⁴ covering over two decades in energy and four decades in beam intensity. The FPCs were required to cover this entire energy range with the general goal of conducting each measurement as quickly as possible while maintaining the lowest possible uncertainty in converting observed counting rates to incident X-ray intensity distributions. These objectives can be stated in terms of lower-level requirements to maximize:

- quantum efficiency (QE),
- collecting area,
- counting rate capacity,
- spectral resolving power,
- spatial scanning capabilities in the focal plane

while minimizing:

- uncertainties in QE (relative and absolute),
- uncertainties in detector collecting area,
- uncertainties in signal-processing deadtime,
- uncertainties in background counting rate,
- performance degradation over time.

In the subsections that follow, the major components of a complete FPC detector system are described, with special attention to how their designs address the above criteria.

2.1. FPC Body

Much of the HXDS hardware design is based on equipment used during the VETA calibration, a preliminary test of the largest AXAF mirror pair conducted in 1991.⁵ Although a mix of sealed and flow proportional counters was used for VETA employing essentially the same bodies as the HXDS FPCs but with smaller windows, concerns about performance degradation in sealed counters and the desire for interchangeability dictated that all seven (and two spare) HXDS proportional counters be nominally identical flow counters.

Because of the large energy range to be covered, the general design philosophy is to use a thin window for good low-energy QE, a deep gas volume for good high-energy QE, and a large window area for good counting statistics in the BNDs. The bodies are constructed of aluminum, with exterior dimensions of 6.50" long by 2.50" wide by 3.35" deep. To prevent high-energy X-rays from producing an extraneous signal from Al-*K* fluorescence, thin (0.008") sheets of beryllium line the back wall and long sides of the inner volume; if an incident photon (or an Ar-*K* escape photon) is not absorbed by the fill gas or Be before it strikes one of the walls, any resulting Al fluorescence photon

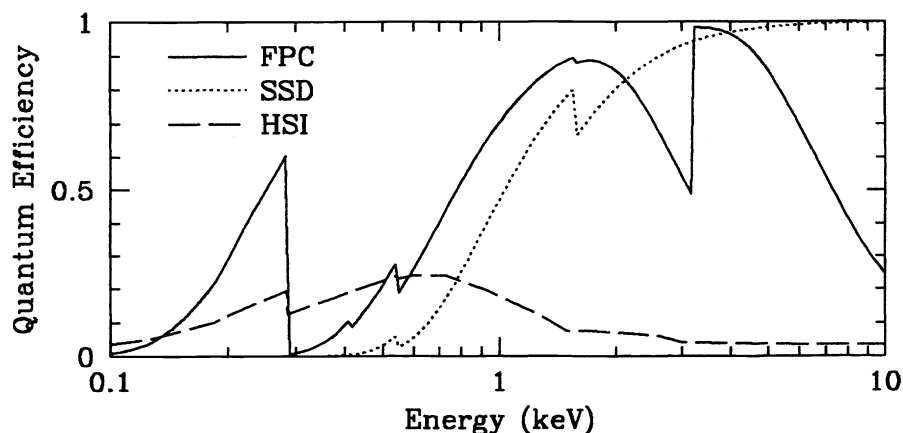


Figure 1. Comparison of FPC, SSD, and HSI quantum efficiencies.

will be absorbed by a Be liner (which has completely negligible fluorescence) before it can enter the active volume of gas.

With the Be liners in place, the active volume of the FPC is 50.4 mm wide and 50.0 mm deep. The window assembly adds another 17.3 mm to the active depth (plus about one mm more in the center of the window because of pressure-induced deflection). A 50- μm -diameter gold-plated stainless steel anode wire runs the length of the FPC, approximately 10 mm closer to the rear Be liner than to the window.

2.2. Window

Each window assembly is constructed of a thin plastic window, made of 1- μm -thick polyimide (nominally $\text{C}_{22}\text{H}_{10}\text{O}_4\text{N}_2$) with a 200- \AA coating of Al on the inside surface (for electrical conductivity), sandwiched between a stainless steel frame and bezel. The window material is epoxied to the frame and supported by a wire grid epoxied to the bezel. The open area of the window is 1.5" by 5.0", although the piece of polyimide is the same size as the frame and bezel, 2.50" by 6.25".

Producing such large pieces of leak-free polyimide was quite a challenge, requiring 8"-diameter pieces of raw material spun on Si wafers.⁶ The requirement for such large single-piece windows was driven by the desire for maximum detector area without the use of multiple "windowpanes," which would create electric field nonuniformities near the window surface and reduce the total open area. In retrospect, a three-pane window design might have provided a better compromise of cost, risk, and performance, but the assembled windows performed extremely well.

Polyimide was chosen over other materials such as polypropylene, beryllium, diamond, and silicon-enriched silicon nitride based on comparisons of such factors as leak-rate, strength, available sizes, ease of handling, and low-energy X-ray transmission.⁷ The window is supported by a grid of 100- μm -diameter gold-coated tungsten wires with 2-mm center-to-center spacing, and is able to withstand a differential pressure of 400 torr with a significant safety margin. Before being mounted on an FPC, each window is leak-tested and pressure-cycled many times. After the initial deformation, the window bowing is very repeatable, with a typical 400-torr deflection of 1.5 mm in the center of the window and 0.3 mm within each 2-mm-square "windowlet."

The 2-mm wire spacing was chosen to minimize uncertainties in the FPC efficiency; although a finer mesh would allow less window bowing, correcting for obscuration of the focused X-ray beam in the focal plane FPC would introduce larger errors. With a distance of 10 mm between each focal-plane aperture and the surface of the central FPC windowlet, focused X-rays spread into rings 1.2-mm in diameter (from the largest AXAF mirror), which fall on the relatively flat central portion of the windowlet except for off-axis measurements. Even so, our extremely tight error tolerances require that detailed models of window deflection, wire obscuration, and (for the focal plane FPC) incident X-ray distribution (in angle and location) be used when analyzing FPC data.

2.3. Gas supply system

Because such thin windows are not entirely leakproof, and because it is desirable to continuously replenish the fill gas in each detector to reduce the buildup of destructive chemicals formed during normal use from electron avalanches, the HXDS proportional counters require a continuous flow of gas. Two Gas Supply Systems (GSSs) are used, one for the BND-500 FPC and one for the four BND-H and two HXDA FPCs. Their function is to control the supply of gas to the FPCs, evacuating and pressurizing the gas lines as necessary, and provide a constant pressure and rate of flow during normal operation.

All measurements use 400-torr P10 gas, a mixture of 90% Ar and 10% CH₄; the Ar provides most of the X-ray opacity while the methane acts as a quench gas, improving the the stability of the electron avalanche. Gas mixtures based on Xe and Kr, which would provide higher QE than Ar at high energies, are not used because of prohibitively higher costs and, in the case of Kr, high background from radioactive contaminants. Pure methane was also investigated for use at low energies because electron diffusion losses (which adversely affect energy resolution) are lower than with argon, but the rate of anode-wire "aging" (discussed below) is orders of magnitude higher. Other quench gases such as ethane, propane, and carbon dioxide can be used with argon, but do not provide better overall performance. Carbon dioxide received particular attention because it slows the anode aging rate, but energy resolution is significantly worse than with methane.

The active elements of the GSSs remain outside the vacuum test chamber, and are connected to the FPCs by flexible stainless steel gas lines. All six of the BND-H and HXDA FPCs are supplied in parallel so that their gas pressures are identical to within 0.1 torr. Absolute pressures were calibrated to ± 0.7 torr using a mercury-filled manometer, with corrections for local gravity and temperature. Pressure stability is maintained to better than ± 0.2 torr via a feedback loop which controls the opening of a gas-supply valve based on pressure-sensor readings. Pressure data and temperature readings from each FPC, accurate to ± 0.10 °C, are logged every forty seconds to enable calculation of the gas density, which is the critical factor affecting QE at high energies where the P10 gas becomes increasingly transparent. These tolerances keep uncertainties in the relative QEs of the FPCs arising from density variations below 0.2%.

The exact composition of the gas mixture also affects QE, and so we use ultra-high purity gas (99.999% pure Ar), with our entire supply filled from the same mixing chamber so that the ratio of argon and methane is identical in each cylinder. Extreme purity was also necessary to minimize the rate of detector degradation from anode aging, which is caused by the buildup of nonconductive deposits on active areas of the FPC anode.⁸ These deposits lead to poorer energy resolution, rate-dependent gain, and eventually electrical breakdown. Some aging is unavoidable since it comes from polymerization of fill-gas molecules as they are ionized and broken apart during normal use, but several other factors can greatly accelerate the process, particularly traces of silicon compounds and, to a lesser extent, chlorine and fluorine. Our gas systems were designed to eliminate these materials, and were scrupulously cleaned before use. Cumulative X-ray exposure was also minimized by blocking the X-ray source when data were not being collected. During the course of AXAF calibration, aging tests were periodically conducted on the focal plane FPC (which received the highest X-ray dose per unit length of anode wire) to look for signs of performance degradation, but none were detected.

2.4. Signal processing electronics

2.4.1. Hardware

Each FPC has its own signal processing chain consisting of: an Ortec 142-PC charge-sensitive preamplifier with 0.15- μ F capacitance, modified for vacuum compatibility; Ortec 671 "Shaping Amplifier," modified for remote control of coarse gain, fine gain, and shaping time constant; and Ortec 921 Multi-Channel Buffer (MCB) analog-to-digital converter. Pulse-height data from the MCBs are transferred via PC server to a Sun UNIX workstation.

Three C.A.E.N. N470 4-channel high voltage power supplies, one each for the BND-500, BND-H, and HXDA, are also remotely controlled by computer (with one PC server per assembly), as are the amplitude settings for three Berkeley Nucleonics Corporation BH-1 Tail Pulse Generators (TPGs). The TPGs feed periodic pulses through each FPC's preamp (to be processed as X-ray events) in parallel with TTL pulses sent to Ortec 994 2-channel Counter/Timers which are gated by the MCBs; comparison of the number of injected pulses with the number of counts in an FPC spectrum's pulser peak permits a precise determination of deadtime. For continuous monitoring

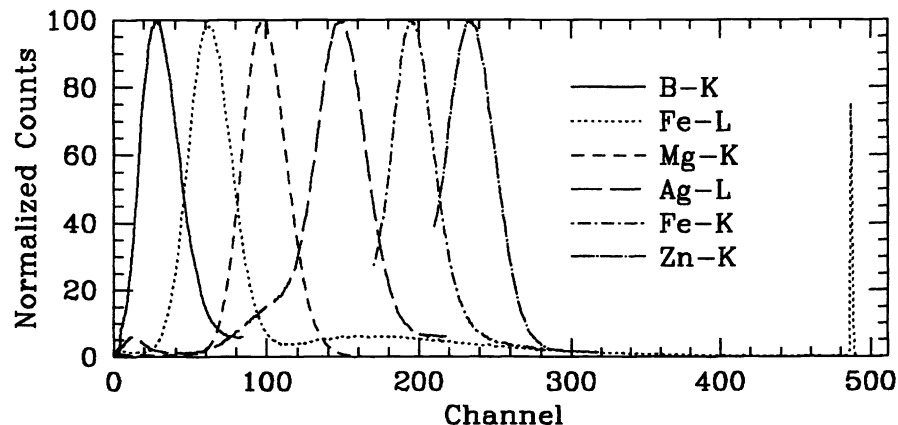


Figure 2. Example FPC pulse height spectra for selected emission lines. With the operational parameters used, only the FPC anode voltage changes with line energy, and peak widths are all approximately the same. The narrow feature near channel 485 is the pulser peak used for deadtime correction.

of counting rates, which is extremely useful for confirming that the source flux is appropriate before opening the HRMA shutters and exposing the focal plane detector, output signals from the shaping amplifiers are also fed into Ortec 850 4-channel Single-Channel Analyzers (SCAs) and then passed along to Counter/Timers, which are read out and logged every ~ 9 seconds.

2.4.2. Voltage and amplifier settings

Settings for the various operational parameters—*anode voltage*, *coarse gain*, *fine gain*, *shaping time constant*, and *lower level discriminator (LLD)*—were chosen to provide pulse-height spectra which were easy to analyze, with as few parameter changes as possible, and to use moderate electron gains so that the rate of anode aging was kept low.

With our chosen compromise, the only setting that needs to be adjusted when X-ray energy changes is the anode voltage, according to the equation $V = -125 \log E + V_0$, where E is the X-ray energy in keV, and V_0 is a voltage which varies slightly with each FPC but is typically 1630 volts. The resulting gas gain from electron avalanches is approximately 20000 at 100 eV and 2000 at 10 keV, scaling as $E^{-1/2}$.

In P10 gas, an average of 28.6 eV is required to create each initial electron-ion pair. Given the gas gain described above, and using a fixed value of 6.54 for the shaping-amplifier gain, with 512 channels to bin the 0-10 volt signals which are fed into the MCB, a 100-eV photon will produce a spectrum with a peak in channel 25 when the FPC voltage is set for 100-eV photons. Since gain scales as $E^{-1/2}$ in this scheme, the position of X-ray peaks scales as $E^{+1/2}$, and so 10-keV X-ray lines appear in channel 250 (when using the 10-keV voltage setting). In proportional counters, energy resolution also scales as $E^{+1/2}$, with a coefficient of ~ 400 eV (FWHM) for P10 gas. The width of X-ray peaks is therefore approximately independent of energy, with a value of about 32 channels, as shown in Figure 2.

This variable-voltage/fixed-amplifier scheme means that continuum background spectra (mostly from cosmic rays) are different for every X-ray energy setting, but low-channel electronic noise is essentially constant, and LLD settings and pulser amplitudes never need to be adjusted. The spectrum cutoff (i.e., the photon energy corresponding to channel 512) also scales as $E^{+1/2}$, thus covering a larger logarithmic energy range at lower energies (where bremsstrahlung continuum from the X-ray source often extends to several times the primary line energy), and a smaller range at higher energies (where the FPCs are much less sensitive to the continuum X-rays).

An alternative method would be to use roughly three voltage/amplifier settings, each spanning a factor of five or so in X-ray energy, but this offers no advantages other than requiring fewer background spectra, and there is always time to collect background data whenever the source energy is changed. With constant amplifier settings (as we

used), it is also easier to spot any changes in the low-channel electronic noise, which may signal electrical interference or other problems. (Note that when the tunable X-ray source monochromators are used, FPC voltages are held fixed over a range of X-ray energy.)

2.4.3. Deadtime determination

The fastest shaping time constant available on the Ortec 671 amplifier is 0.5 μsec , with a net signal processing time (when used with the Ortec 921 MCB) of $\sim 5.8 \mu\text{sec}$. We chose this setting because longer shaping times do not produce any noticeable improvement in energy resolution, and because we desire a high counting rate capacity, which requires short shaping times. During AXAF calibration we rarely exceeded 20000 Hz, which corresponds to a deadtime of $\sim 13\%$.

Although the Ortec 921 MCBs have sophisticated pileup rejection circuitry and utilize the Gedke-Hale deadtime-correction algorithm, our own calibration experiments (described in section 3) have shown that the true system deadtime can differ from the MCB estimate by several percent (e.g., 8.5% vs. 5.7%), particularly when the LLD setting is not far above the level of the electronic noise. We therefore use the periodic-pulsar deadtime-correction method, in which regularly timed pulses are injected into the test input of the FPC preamplifier. (To minimize the number of electronics modules, we use one pulser to feed all four BND-H FPCs in parallel.) Those pulses are then processed as X-ray events and appear in the FPC spectrum as a narrow peak, with the pulser amplitude chosen so that the peak appears near channel 480, away from most or all of the X-ray spectrum. The number of counts in that peak is compared with the number of injected pulses and their quotient is, to first order, the detector livetime. Higher-order corrections, including an adjustment for signals that fall below the LLD but take time to process (the main weakness of the Gedke-Hale algorithm), permit determination of deadtime to a typical accuracy of 0.2%, generally limited by statistical uncertainties in the number of pulser peak counts. We use a pulser rate of 300 Hz, which provides adequate statistics for all AXAF calibration measurements using the FPCs, so that deadtime errors are never the limiting factor in overall measurement accuracy. The same method is used with the SSDs.

2.5. Apertures

Each FPC has a blocking plate mounted on top of its window assembly, with "knife edges" to prevent X-ray reflections. On the four BND-H FPCs, these blocking plates, made of 1/8"-thick stainless steel with open areas 100 mm long and 37 mm wide, serve as the apertures, except for the mapping FPC which has an additional 36-mm-diameter aperture which can be flipped into position. The rectangular apertures are slightly shorter than the full window size (125 mm) because gas gain is somewhat higher at the two ends of the FPC. This effect, caused by electric field nonuniformities around the finite-length anode wire, is very consistent from one FPC to another and could be modeled during spectral fitting analysis, but it is easier to simply block the ends and expose only the flat-gain portion of the detector.

The BND-500 FPC offers more flexibility in beam intensity monitoring, as it has four selectable apertures with diameters of 36, 12, 4, and 1 mm. A blocking plate, with 37-mm-diameter hole, ensures that only one aperture is exposed at a time. Although its collecting area is much less than that of the BND-H FPCs, it is more than thirteen times closer to the X-ray source, so one of its apertures always provides an appropriate counting rate. Indeed, there were many occasions when it was the only FPC capable of monitoring the source; when very low X-ray fluxes were used, as when calibrating the flight detectors, the BND-H FPCs had very poor signal-to-noise ratios, and at extremely high fluxes they sometimes had to be turned off to avoid overexposure.

The focal plane FPC has an Aperture Plate, filled with twenty circular apertures, ranging from 3 μm to 35-mm in diameter, and fourteen slits (designed for grating and Ring Focus measurements), ranging between 5 and 500 μm wide. The Aperture Plate can be moved horizontally and vertically with respect to the FPC so that any aperture can be centered on the midpoint of the FPC, directly in front of a 37-mm-diameter opening in the blocking plate. Apertures less than 1 mm across were made from gold foil (mounted in stainless steel holders) because conventional machining methods could not be used. Instead, apertures between 30 and 500 μm in size were fabricated with laser drilling, and the smallest apertures (less than 30 μm across) used focused ion beam milling. Gold foil was used because it is quite effective at blocking X-rays even when very thin, and because it is relatively easy to work with.

With small apertures, the dimensions of the open area are comparable to or smaller than the thickness of the gold foil of which they are made. To reduce the effect of X-ray reflections and scattering off the side walls of the aperture hole, the foil is as thin as possible, consistent with requirements for X-ray opacity. For apertures less than

25 μm across, the gold foil is only 12.5 μm thick, which can only be used below about 6 keV because it becomes increasingly transparent. In practice, this is not a problem because it is not important to measure the HRMA focus on very small scales at high energy; thicker apertures are also available on the focal plane SSD if needed.

3. DETECTOR CALIBRATION

Although preliminary FPC calibration in all the areas listed below has been completed, mostly at the HXDS “Pipe” facility, the accuracy of those measurements generally does not meet our requirements. Followup calibration involves measurements at the Pipe, the XRCF (summer 1997), and the BESSY synchrotron in Berlin (winter 1997/98).

3.1. Spectral response function

In order to extract the precise number of X-rays events from an FPC spectrum, we use a detailed spectral fitting program, implemented within the XSPEC suite.^{9,10} One requirement for such spectral fitting is an accurate model of the spectrum produced from a monochromatic X-ray line, called the spectral response function (SRF), at all energies. The best way to obtain a spectrally pure line is from a synchrotron with a monochromator, with appropriate filters or “cut-off mirrors” to block higher orders if necessary. These measurements will be conducted at the BESSY synchrotron using their low-energy SX-700 grating monochromator and the higher-energy KMC double-crystal monochromator. At least 10^6 counts will be collected at each of several energies, mostly below 1 keV, which will allow adequate characterization of the low-energy “shelf” (mostly from electron diffusion losses to the window) and the high-energy “tail.”

As mentioned previously, the gas gain is not uniform over the entire length of the anode wire, which is why we use BND-H apertures which are not as long as the window openings. Even over this region, the gain is a few percent higher at the ends of the exposed region than in the middle, which manifests itself in the BND-H FPCs as a slightly broader SRF than for the BND-500 and focal plane FPCs. Since the synchrotron beam used to calibrate the SRFs is at most only a few mm across, the effect of this spatial gain nonuniformity (previously calibrated on the HXDS Pipe) will be included in our models of the SRF.

3.2. Quantum efficiency

3.2.1. Relative vs. Absolute

One of the goals of AXAF calibration is to measure the effective area of AXAF (with all combinations of mirrors, gratings, and flight detectors) to about 2% (somewhat better for the HRMA alone, and somewhat worse for the gratings), which requires knowing the absolute QE of the BND FPCs to about 1%.¹¹ At lower energies, where the P10 gas is opaque, QE is essentially determined by window transmission, so we will calibrate one or two detached FPC windows at the BESSY synchrotron this winter, measuring transmission at several energies (using a monochromator) to a fraction of one percent at a representative sample of points. At higher energies, gas opacity becomes the dominant factor in QE, and at all energies there are small but difficult-to-model effects such as charge diffusion losses and details of photoionization, quenching, and escape peaks. We therefore also will measure the net QE of an assembled FPC, relying on the absolute intensity calibration of the BESSY X-ray beam. At some energies, the efficiency of the monochromators is known well enough to make measurements at discrete energies, but we will also make measurements using a “white beam” (for which the absolute intensity can be calculated to much better than 1%) in combination with several precisely-calibrated filters to select various energy bands.

For measurements of effective area without the flight detectors, we can achieve even better accuracy because we are comparing the number of detected X-ray events in virtually identical detectors. Systematic errors, such as uncertainties in spectral-fitting results and gas pressure, largely cancel out when comparing data from the normalization and focal plane FPCs, and so our error budget allows only $\sim 0.3\%$ uncertainty in the relative QEs of the BND and HXDA detectors. Relative calibration of all FPCs (and SSDs) will be completed at the XRCF this spring and summer, during and following “flat-field” testing of the ACIS. In these tests, the detectors are exposed to the X-ray beam without the HRMA in place; small spatial variations in beam intensity, on the order of one or two percent and caused by nonuniformities in the the source filter, are measured by the two mapper FPCs.

3.2.2. Window bowing and wire support

Flat-field tests provide information on the relative QE of detectors when exposed to uniform, normal-incidence X-rays, but during AXAF calibration the HXDA FPC was exposed to focused X-rays arriving over a range of angles with a very nonuniform intensity distribution. Detector calibration must therefore include study of the effects of window bowing and obscuration by support wires. These effects must also be included in models of the BND-500 FPC, which uses several apertures, thus exposing different regions of the window. Most of these studies will be conducted at BESSY, using its high-intensity X-ray beam to map out variations in QE on small scales (typically 0.5 mm), around and between the window support wires. The results will be used to parameterize theoretical models of how the polyimide bows around and between the support wires, so that the effective QE of the focal plane FPC can be calculated for any combination of X-ray energy, mirror, mirror orientation, grating order, and aperture size.

3.3. Deadtime

The allowable uncertainty in detector deadtime is $\pm 0.25\%$. As described earlier, we use the periodic-pulsar method with our FPCs and SSDs, which have exactly the same signal processing systems, apart from their preamplifiers. For practical reasons, we have broken our calibration tests into two pieces: deadtime consistency and counting rate linearity.

Consistency tests were conducted using an ^{55}Fe radioactive source and an SSD, with the source placed under vacuum at a fixed distance. We compared net counting rates (after correcting for source half-life, sub-LLD electronic noise, pileup, pulser-pulsar noninterference, and higher-order effects) using many different combinations of pulser rate, shaping time constant, and LLD and demonstrated that the computed rate was the same in each case to within statistical limits, typically less than 0.1%. The computed rate also agreed with the rate derived using a "truly" random pulser method, in which pulses were triggered by radioactive decays. These tests and the deadtime-correction equations we used will be described in a future paper.

Because our detectors cover such a large range in counting rate, we must also calibrate their linearity. We will do this at the BESSY synchrotron, where relative beam intensity can be determined to $\sim 0.1\%$, even when using monochromators. The tests will be conducted using both an FPC and SSD.

3.4. Aperture areas

The areas of large apertures, such as the BND blocking plates and focal plane apertures larger than about 1 mm, can be measured to the required accuracy (about 0.2%) using mechanical means. For focal plane apertures between 1 mm and about 100 μm , we will make measurements of relative areas on the HXDS Pipe facility using X-rays, comparing normalized counting rates with the apertures placed in front of an FPC. For even smaller apertures, the X-ray flux available at the Pipe is insufficient to yield adequate counting rates with such small areas, and we will make relative area measurements at the BESSY synchrotron, with its bright beam. Slight variations in intensity across the beam will be measured when necessary. The BESSY measurements will be made at several energies to calibrate the energy dependence of each aperture's effective area, which arises from reflections off the side walls of the hole. The magnitude of the expected energy dependence is not well known, but based upon AXAF calibration results it does not appear to be more than a few percent. Accuracy requirements vary with aperture size, but are typically about one percent for the small apertures.

ACKNOWLEDGEMENTS

We wish to thank the entire Smithsonian HXDS team, particularly Tim Norton, Paul Okun, Dick Goddard, and John Moran for their expertise in designing and building the HXDS detector assemblies and software system. The support of the High Energy Astrophysics Division and AXAF Mission Support Team, particularly Dan Schwartz, is gratefully acknowledged, as are our many conversations with Jeff Kolodziejczak, Jiahong Juda, and Dick Edgar. This work was performed under the auspices of the National Aeronautics and Space Administration by the AXAF Mission Support Team under Contract No. NAS8 40224.

REFERENCES

1. S. Kraft, F. Scholze, R. Thornagel, G. Ulm, W. C. McDermott, and E. M. Kellogg, "High-accuracy calibration of the HXDS HPGe detector at the PTB radiometry laboratory at BESSY," in *EUV, X-Ray, and Gamma-Ray Instrumentation for Astronomy VIII, Proc. SPIE 3114-06*, 1997.
2. W. C. McDermott, E. M. Kellogg, B. J. Wargelin, S. A. Vitek, E. Y. Tsiang, D. A. Schwartz, R. Edgar, S. Kraft, F. Scholze, R. Thornagel, G. Ulm, M. Weisskopf, S. Odell, A. Tennant, and J. Kolodziejczak, "AXAF HXDS germanium solid state detectors," in *Grazing Incidence and Multilayer X-ray Optical Systems, Proc. SPIE 3113-61*, 1997.
3. I. N. Evans, E. M. Kellogg, W. C. McDermott, M. P. Ordway, J. M. Rosenberg, and B. J. Wargelin, "High-speed imager AXAF calibration microchannel plate detector," in *Grazing Incidence and Multilayer X-ray Optical Systems, Proc. SPIE 3113-02*, 1997.
4. J. J. Kolodziejczak, R. A. Austin, R. F. Elsner, M. K. Joy, M. Sulkanen, E. M. Kellogg, and B. J. Wargelin, "X-ray source system at the MSFC x-ray calibration facility," in *X-Ray and Extreme Ultraviolet Optics, Proc. SPIE 2515*, pp. 420–435, 1995.
5. W. A. Podgorski, K. A. Flanagan, M. D. Freeman, R. E. Goddard, E. M. Kellogg, T. J. Norton, J. P. Oullette, A. G. Roy, and D. A. Schwartz, "VETA-I x-ray detection system," in *Multilayer and Grazing Incidence X-ray/EUV Optics for Astronomy and Projection Lithography, Proc. SPIE 1742*, pp. 40–54, 1992.
6. F. R. Powell, R. A. M. Keski-Kuha, M. V. Zombeck, R. E. Goddard, G. Chartas, L. K. Townsley, J. M. Davis, and G. M. Mason, "Metalized polyimide filters for x-ray astronomy and other applications," in *Grazing Incidence and Multilayer X-ray Optical Systems, Proc. SPIE 3113-47*, 1997.
7. T. H. Markert, J. M. Bauer, C. R. Canizares, T. Isobe, S. Nenonen, J. O'Connor, and M. L. Schattenburg, "Proportional counter windows for the Bragg Crystal Spectrometer on AXAF," in *EUV, X-Ray, and Gamma-Ray Instrumentation for Astronomy II, Proc. SPIE 1549*, pp. 408–419, 1991.
8. J. A. Kadyk, "Wire chamber aging," *Nuclear Instruments and Methods in Physics Research A* **300**, pp. 436–479, 1991.
9. R. J. Edgar, E. Y. Tsiang, A. Tennant, S. Vitek, and D. Swartz, "Spectral fitting in AXAF calibration detectors," in *Grazing Incidence and Multilayer X-ray Optical Systems, Proc. SPIE 3113-12*, 1997.
10. E. Y. Tsiang, R. J. Edgar, A. Tennant, S. A. Vitek, and E. M. Kellogg, "JMKMOD: a software suite within XSPEC for the ground calibration of AXAF," in *Grazing Incidence and Multilayer X-ray Optical Systems, Proc. SPIE 3113-14*, 1997.
11. E. M. Kellogg, *et al.*, "Absolute calibration of the AXAF telescope effective area," in *Grazing Incidence and Multilayer X-ray Optical Systems, Proc. SPIE 3113-59*, 1997.